# Intramolecular Charge Transfer Probe Induced Formation of α-Cyclodextrin Nanotubular Suprastructures: A Concentration Dependent Process

**ARTICLE** *in* THE JOURNAL OF PHYSICAL CHEMISTRY C · JULY 2008

Impact Factor: 4.77 · DOI: 10.1021/jp8018952



**5 AUTHORS**, INCLUDING:

Pradipta Purkayastha

Indian Institute of Science Education and …

**73** PUBLICATIONS **819** CITATIONS

SEE PROFILE

# Intramolecular Charge Transfer Probe Induced Formation of α-Cyclodextrin Nanotubular Suprastructures: A Concentration Dependent Process

**S. Syed Jaffer,[†] Subit Kumar Saha,[†] G. Eranna,[‡] Ashok K. Sharma,[‡] and Pradipta Purkayastha*,[†]**

*Department of Chemistry, Birla Institute of Technology and Science, Pilani 333031, Rajasthan, India, and Sensors and Microsystems Group, Central Electronics Engineering Research Institute, Pilani 333031, Rajasthan, India*

*Received: March 4, 2008; Revised Manuscript Received: May 24, 2008*

A suitably sized charge transfer probe of an elongated geometry can induce the formation of α-cyclodextrin nanotubular suprastructures, a rare event because of size restriction of the host. The specific molecular structure is found to be responsible only for the 1:2 guest−host complex formations. No evidence of the formation of the 1:1 complex is found. Steady-state fluorescence anisotropy and atomic force microscopy show that the nanocomposites club with other such species very efficiently to form nanotubes and nanoclusters because of primary interactions through hydrogen bonding and develop nanotubular suprastructures due to secondary interactions. The degree of formation of the suprastructures is found to be very much controlled by the probe concentration. In aqueous environment, 2 $\mu$M is observed to be the best concentration for the fluorophore form of large rodlike aggregates. Concentrations as low as 1 $\mu$M and as high as 4 $\mu$M induce the formation of relatively smaller structures. The findings encourage the applications of cyclodextrin nanotubular clusters toward nanotechnology and pharmaceutical research. The concentration dependent phenomenon will dictate the drug dosage as also the extent of formation of the nanostructures in the formation of insulated nanowires. The work is purely indicating the anchoring capability of the used molecule to form nanotubular α-CD suprastructures which otherwise does not form so frequently.

## Introduction

The fundamental concept for the spontaneous formation of supramolecular architecture with well-defined structure and functionality by molecular self-assembly can be exemplified by protein aggregation, membrane formation, polymerization, nanotube formation, etc.[1] Complexes of organic compounds with cyclodextrins are appropriate models to study the process of molecular self-assembly.[2] Enzymatic degradation of starch using a glycosyl transferase from *Bacillus macerans* yields cyclodextrins biotechnologically.[3] They belong to a homologous cycloamylose series of cyclic oligomers consisting of six to nine α-1,4-linked D-glucopyranosyl residues. The six-, seven-, and eight-membered residues, viz., α-, $\beta$-, and $\gamma$-cyclodextrins (α-CD, $\beta$-CD, and $\gamma$-CD) have been the focus of interest to researchers in pure and applied fields.[3,4] The hydrophobic inner cavity of the truncated conelike structures of the CDs have 4−8 Å diameter. It is well known that cyclodextrin and its derivatives can incorporate appropriately sized guest molecules selectively through weak interactions like hydrophobic interaction, van der Waals force, and hydrogen bonding.[5] Depending on the relative sizes of the cyclodextrins and the guest molecules, more than one guest can be accommodated inside a single CD cavity.[6] If the guest molecule is long enough, several cyclodextrins can be threaded along its length.[7] Formation of compound-induced cyclodextrin nanotubes or nanorods has been the topic of interest for many groups in the applied field of chemical research. Starting from some of the preliminary works of Li et al. and Pistolis et al.[2] advancement in the research on the formation of these suprastructures has continued to bring interest to many workers. In most of these cases, formation of well-structured nanorods has been observed with $\beta$- and $\gamma$-CDs because of their ample cavity space compared to that for α-CD.[2,8] Cyclodextrin-based aggregates have been widely investigated with microscopies such as STM, AFM, SEM, TEM, and fluorescent microscopy to obtain the direct morphology and structure of samples.[9] He et al. talked about various types of cyclodextrin aggregates, inclusion complexes and their aggregates of cyclodextrin rotaxanes and polyrotaxanes, cyclodextrin nanotubes and their secondary assembly.[9] Miyake et al. explained the formation process of cyclodextrin necklace through the analysis of hydrogen bonding on a molecular level.[9] They reported that most CDs are arranged in head-to-head or tail-to-tail conformation through secondary−secondary or primary−primary hydrogen bonding, respectively. However, nanotube and nanorod formation of α-CD has also been observed, although the studies are comparatively much less than $\beta$- and $\gamma$-CDs. α-CD-based self-assembled nanotubes have been reported to form at the air−water interface[10] as also can be threaded by polyethylene glycols.[7,11] In all these works, stable α-CD nanotubes could only be developed either on well-defined surfaces or using polymeric molecules to hold them together. Unlike $\beta$- and $\gamma$-CDs, formation of molecule-induced stable α-CD nanotubes could not be observed so frequently, probably because of the size factor and consequently the thermodynamic instability of the complexes (see Supporting Information for the theoretically calculated molecular dimensions of DMASBT).

In the present communication, we have attempted to explain the method of construction of α-CD nanotubular suprastructures with the aid of a twisted intramolecular charge transfer (TICT) probe trans-2-[4-(dimethylamino)styryl]benzothiazole (DMAS-

* Corresponding author. E-Mail: prad_purk@yahoo.com.
[†] Birla Institute of Technology and Science.
[‡] Central Electronics Engineering Research Institute.

10.1021/jp8018952 CCC: $40.75 
Published on Web 07/08/2008

**SCHEME 1: Representative Structure of DMASBT**[a]

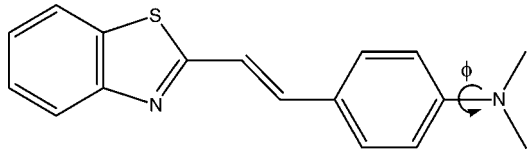


[a] $\phi$ indicates the twist angle of the -N(CH$_3$)$_2$ moiety with respect to the rest of the molecule.

BT) (Scheme 1). Development of cyclodextrin-covered organic nanotubes and their suprastructures induced by the self-assembly of dendrons uses the $\beta$- and $\gamma$-CD cavities.[13] Large molecules, like the dendrons, thus have been proven to act as good foundation to induce the nanotube formations that can develop further to adopt the supramolecular structural motifs. The TICT probes show a highly Stokes-shifted fluorescence band in polar solvents, which develops as a result of twisting of the donor part around the single bond connecting the donor to the acceptor system of the molecule in the excited state.[13] Exploiting this characteristic feature, these molecules have been extensively used to probe the microheterogeneous biomimicking environments developed by micelles, reverse micelles, cyclodextrins, etc.[14] The compound, DMASBT, is one of those TICT probes, but it has been specially chosen in this case because of its elongated structural nature so that it can effectively attempt to promote the formation of cyclodextrin nanotubes through 1:2 probe-CD complexation.

## Experimental Section

**Materials.** DMASBT was procured from Aldrich Chemical Co., WI and was recrystallized from a mixture of ethanol and small percentage (~10%) of *n*-hexane. Triple distilled water was used for the preparation of aqueous solution. Stock solution of DMASBT ($1.001 \times 10^{-3}$ M) was prepared in pure methanol, 0.1 mL of which was poured in a 10 mL volumetric flask and left for a few hours for complete evaporation of methanol before dissolving in water containing appropriate concentration of α-CD. The final volume of the solution was 10 mL, and the final concentration of DMASBT was $1 \times 10^{-5}$ M. α-CD was procured from Sigma-Aldrich, WI and was used as obtained. Potassium iodide was procured from Merck, India.

**Methods.** The absorption spectra were recorded using a Jasco V570 UV−vis spectrophotometer. Fluorescence measurements were performed using a Shimadzu RF-5301PC scanning spectrofluorimeter. The fluorescence lifetimes were measured by the method of time-correlated single-photon counting and a picosecond spectrofluorimeter (Edinburgh Instrument, 199) was used for the purpose. A nano-LED pulsed diode powered by a pulsed diode controller (IBH) was used as the excitation light source. The excitation wavelength was 403 nm. The typical response time of this laser system was 70 ps. To calculate the lifetime, the fluorescence decay curves were analyzed by an iterative fitting program provided by IBH.

The steady state fluorescence anisotropy measurements were performed with the same Shimadzu (RF-5301PC) spectrofluorimeter fitted with a polarizer attachment. The steady state anisotropy, $r$, can be represented as $r = (I_{VV} - GI_{VH})/(I_{VV} + 2GI_{VH})$, where $I_{VH}$ and $I_{VV}$ are the intensities obtained from the excitation polarizer oriented vertically and the emission polarizer oriented in horizontal and vertical orientations, respectively. The factor $G$ is defined as $G = I_{HV}/I_{HH}$. The AFM experiments were done using a Nanoscope II instrument (Digital Instrument Inc., USA) with lateral resolution of 1 Å and vertical resolution of 0.1 Å fitted with a Au-coated probe. The surface for the sample spread was made of highly oriented pyrolytic graphite (HOPG). The theoretical calculations were done by the semiempirical AM1 method using HyperChem 6.0 (Hypercube Inc., Canada). The ground state ($S_0$ geometry) of the compound was optimized by AM1 method. AM1-SCI (singly excited configuration interaction) was performed to get the energy ($E_g$) and dipole moment in the ground-state and the transition energies ($\Delta E_{i\rightarrow j}$), and dipole moments of different excited states. We have taken care of all the singly excited configurations within an energy window of 11 eV from the ground state. $\Delta E_{i\rightarrow j}$ corresponds to the excitation of an electron from the orbital $\phi_i$ (occupied in the ground state) to the orbital $\phi_j$ (unoccupied in the ground state). The total energy of the excited state ($E_j$) was then calculated as $E_j = E_g + \Delta E_{i\rightarrow j}$. The CI wave function has been used to generate g orbitals and one-electron density matrices, which were used to calculate the dipole moments of the excited states of the compound.

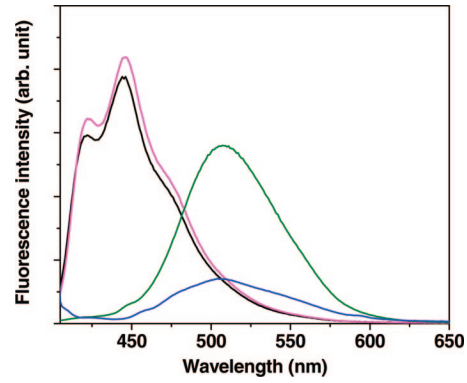


**Figure 1.** Fluorescence spectra of DMASBT in hexane (black), heptane (magenta), methanol (green), and 8:2 water−methanol mixture (blue) as solvents ($\lambda_{exc}$ = 395 nm, [DMASBT] = $1 \times 10^{-5}$ M).

## Results and Discussion

DMASBT has dual fluorescence. This characteristic feature of the compound (as explained later) can be exploited very effectively to monitor the probe-CD interaction. The absorption spectrum of DMASBT shows a maximum at ~400 nm. On excitation at 395 nm the locally excited (LE) fluorescence appears at ~448 nm with its characteristic structural features. In solvents of high polarity, the TICT fluorescence comes with a band maximum at around 510 nm (8:2 water−methanol mixture) (Figure 1).[15] The band maximum shifts to ~530 nm in aqueous solution containing only 1% methanol (see inset of Figures 2 and 3). The LE band is more pronounced in solvents of lower polarities. The TICT state (twist angle ($\phi$) = 90°) of DMASBT has a large dipole moment and undergoes a large degree of solvation in solvents with higher polarities and as a consequence yields a red-shifted fluorescence at ~510 nm.[15] If the compound can undergo total or partial encapsulation in the hydrophobic cavity of cyclodextrin, the solvation of the TICT energy state shall decrease and the fluorescence band will suffer a blue shift. This hypsochromic shift will pose as a direct proof of encapsulation of the probe within the hydrophobic nanocavity of cyclodextrin.

Cyclodextrin can undergo complexation with guest molecules in different ways. Depending upon the type of cyclodextrin used (α-, $\beta$-, or $\gamma$-), the guest molecule orients itself so as to have effective encapsulation with the host.[16] The hydrophobic cavity of the cyclodextrin invites the organic molecules to reside in them either loosely fitted or tightly trapped depending on the

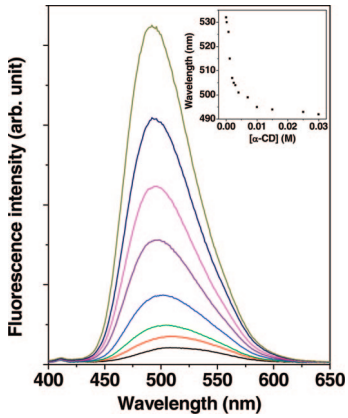


**Figure 2.** Fluorescence spectra of DMASBT (2 $\mu$M) in different concentrations of α-CD: (black) 1.2 mM; (red) 2 mM; (green) 3 mM; (blue) 4 mM; (purple) 7 mM; (magenta) 10 mM; (navy blue) 15 mM; and (olive) 30 mM. The inset is showing the positions of the fluorescence maxima with increasing concentration of α-CD ($\lambda_{exc}$ = 360 nm).

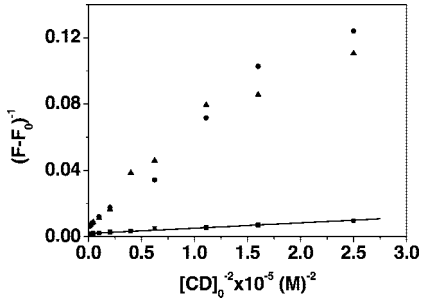


**Figure 3.** Plot of $1/(F - F_0)$ against $1/[CD]_0^2$ for 1 $\mu$M (■), 2 $\mu$M (•), and 4 $\mu$M (▲) DMASBT in α-CD. The linear fit to the data for 1 $\mu$M DMASBT is shown in the figure.

cavity size. As mentioned earlier, both 1:1 as well as 1:2 probe-CD complexation is frequently observed. The nature and structure of the DMASBT molecule seems to be very much favorable to undergo such complex formation. The absorption spectra of DMASBT at different concentrations of α-CD show an isosbestic point at 360 nm indicating the formation of a second species (probe-CD complex in this case) in solution. DMASBT was thus excited with a light of wavelength 360 nm where the absorption coefficient of both the species is the same. The blue shift in the fluorescence spectra of DMASBT with increasing α-CD concentration indicates obvious encapsulation (Figure 2). The point to chase after this is to understand the nature of complexation. A simplified and straightforward method to determine the stoichiometry of the probe-CD complexes along with the equilibrium constant is the double-reciprocal plot as described by the following equations for 1:1 (eq 1) and 1:2 (eq 2) complexation, respectively[2,17,18]

$$\frac{1}{F - F_0} = \frac{1}{F_m - F_0} + \frac{1}{K[CD]_0(F_m - F_0)} \quad (1)$$

$$\frac{1}{F - F_0} = \frac{1}{F_m - F_0} + \frac{1}{K'[CD]_0^2(F_m - F_0)} \quad (2)$$

Here, $F_0$ and $F_m$ are the fluorescence intensities at zero and the maximum concentrations of α-CD, $F$ denotes the fluorescence intensities at different concentrations of α-CD, $[CD]_0$ is the total CD concentration, and $K$ and $K'$ are the binding constants. The slope of the linear fit to $1/(F - F_0)$ versus $1/[CD]_0$ or $1/[CD]_0^2$ with a positive intercept gives the stoichiometry and

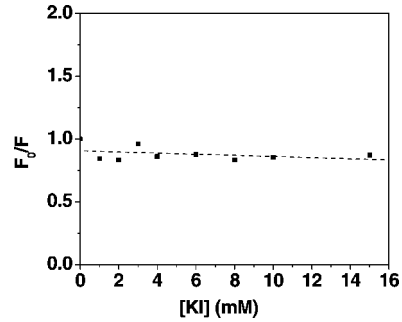


**Figure 4.** Fluorescence quenching of α-CD-DMASBT in $H_2O$ by $I^-$ ion. $F_0$ denotes the fluorescence of DMASBT in absence of KI and $F$ denotes that in presence of different concentrations of the quencher ([DMASBT] = 2 $\mu$M, [α-CD] = 10 mM, $\lambda_{exc}$ = 360 nm, $\lambda_{em}$ = 500 nm).

the slope of the line gives the binding constant. It is important to mention here that $[CD]_0$ should be the free concentration of cyclodextrin, which is, as such, unknown. As a general practice, the total concentration of host added at each stage is used as $[CD]_0$. Adopting a self-consistent approach one can resolve this problem. In the first stage, one can determine $K$ using the total cyclodextrin concentration as $[CD]_0$.[19] Taking this solution, one can easily calculate for 1:1 association concentrations of the cyclodextrin in the free and bound state. In the second stage, one can redetermine $K$ using this free host concentration as $[CD]_0$. This ultimately leads to a self-consistent value of the association constant $K$.[19] However, this method is not suitable for the systems where there is a possibility of nanotube formation, since this is a multistep process.[2]

In our study we endeavored to excavate the impact of the probe concentration on the formation of the host−guest complex. For that purpose, we used three different DMASBT concentrations, viz., 1, 2, and 4 $\mu$M. In all these three cases, we observed the hypsochromic shift in the fluorescence spectra that confirmed encapsulation. However, the double reciprocal plot failed to show any hint of formation of 1:1 probe-α-CD complex (no linear fit obtained). This could be obvious because of the structural characteristic of DMASBT. α-CD has the smallest cavity size among the other CDs and the dimensions of DMASBT do not allow it to go much inside of the cavity. Hence, due to the exposed bulk of the molecule, the 1:1 probe-α-CD complex becomes thermodynamically unfavorable. So, the most probable motif of encapsulation is 1:2, where the probe molecule is held by two molecules of α-CD from the two ends. The double-reciprocal plot for 1:2 complexation indicates the presence of such complexes with a DMASBT concentration of 1 $\mu$M. The binding constant comes out to be 60 248.45 $M^{-2}$ ($R$ = 0.998). However, this method fails for the higher concentrations (2 and 4 $\mu$M) of DMASBT indicating a multistep process. From the earlier reported works on $\beta$- and $\gamma$-CDs, we presume that DMASBT is inducing the formation of CD nanotubes at these concentrations. Before we proceed further, it is pertinent to give evidence for the adequate protection of DMASBT by the formation of the nanotubes. For this purpose, we applied increased concentration of $I^-$ ions in the probe-CD solution to observe any quenching of fluorescence that is obvious if there is any 1:1 complex formation and/or no complexation. The fluorescence of bare DMASBT undergoes progressive quenching by increasing concentration of potassium iodide (KI). The Stern−Volmer constant for the process is found to be 69.79 $M^{-1}$. We could not find any such quenching of DMASBT in presence of α-CD but could find the evidence of adequate protection of DMASBT by the CD buckets (Figure 4).

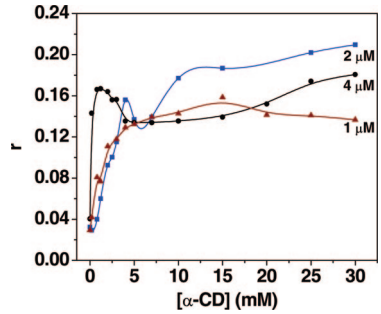


**Figure 5.** Plot of change of the steady-state fluorescence anisotropy ($r$) of DMASBT in different α-CD concentrations ($\lambda_{exc}$ = 360 nm, $\lambda_{em}$ = 500 nm, the $r$ values have been measured with an error of ± 0.01).

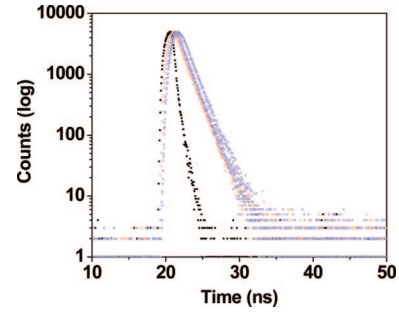


**Figure 6.** Fluorescence decay profiles for different concentrations of DMASBT (red circle, 1 μM; purple triangle, 2 μM; blue inverted triangle; 4 μM, and ■, probe lamp profile) in α-CD.

**TABLE 1: Decay Parameters of DMASBT in 10 mM α-CD Solution**

| [DMASBT] (μM) | $\tau_1$ (ns) | % contribution | $\tau_2$ (ns) | % contribution | $\chi^2$ [a] |
|---|---|---|---|---|---|
| 1 | 0.94 | 66 | 1.48 | 34 | 1.15 |
| 2 | 1.16 | 82 | 1.88 | 18 | 1.20 |
| 4 | 0.24 | 67 | 1.38 | 33 | 0.96 |

[a] $\chi^2$ values have been given instead of the fit residuals for clarity and to save space.

The motional restrictions of entrapped or encapsulated compounds can be well accounted by the steady-state fluorescence anisotropy measurements.[20] Experiments in 100% glycerol medium showed that the $r_0$ value for DMASBT is 0.38. The anisotropy plots of different concentrations of DMASBT with increasing concentration of α-CD is shown in Figure 5. Increasing α-CD concentration in a solution of 1 μM probe concentration dictates a gradual increase in the steady-state fluorescence anisotropy ($r$) from a low value of ∼0.03 to a higher value of ∼0.13 with very little disturbance due to less further rearrangements of the smaller aggregates. On increasing the probe concentration to 2 μM, the $r$ plot with the α-CD concentration does not behave as the previous case. The plot can be easily separated into three phases. In the first phase, $r$ increases to ∼0.16 that can be correlated with the normal 1:2 encapsulation of the guest in the host (α-CD) and formation of small nanoaggregates. In the second phase, a 0.025 unit decrease in the $r$ value is noted at around 4 mM α-CD concentration, which indicates some abnormality in the arrangement of the complexes swimming in the bulk aqueous environment. This is immediately followed again by an increase in the $r$ value to more than 0.2 at an α-CD concentration of 30 mM. This peculiarity in the plot is an obvious indication of further rearrangement of the formed minute complexes pointing toward there self-aggregation to form bigger nanotubes followed by nanotubular suprastructure formation. Although only with these observations it is still too early to talk about the suprastructure formations, but at least we could get some indications for further research on this matter. From here onward it looks quite plain and simple that with increasing DMASBT concentration the potentiality of the nanoaggregate formation increases. Following this presumption, similar experiments were performed with a higher concentration of DMASBT (4 μM). The anisotropy plot appeared to be somewhat different compared to that in the case of 2 μM DMASBT. The $r$ value increased sharply to 0.17 at 2 mM α-CD concentration. This event is followed by similar lowering in the $r$ value as was observed in the case of 2 μM DMASBT. But surprisingly, the next event does not match with that seen in the previous case. The $r$ value increased very slowly in contrary to that observed in the former. This clearly indicates that the intermediate concentration of 2 mM α-CD is the best option for the development of bigger nanotubular aggregates.

To develop a better view about the changes in the photophysics of the probe molecule in different concentrations in the α-CD environment, we performed some time-resolved fluorescence experiments. As it is already well known that the fluorescence decay is directly related to the motional restriction of the fluorophore, our proposition for the formation of the nanotubular aggregates can be well examined by exploiting this fact. As per the anisotropy data, DMASBT must exhibit a double exponential decay witnessing the presence of more than one species in the solution. Moreover, the decay rate should be the slowest at a DMASBT concentration of 2 μM, the intermediate probe concentration that favors the formation of bigger nanotubular aggregates compared to the other experimental probe concentrations. Figure 6 demonstrates the fluorescence decay profiles of DMASBT present in different concentrations at a particular concentration of α-CD (10 mM) where the tubular aggregation is supposed to have developed. Table 1 shows the fluorescence decay times of different concentrations of DMASBT in 10 mM α-CD. $\tau_1$ represents the fluorescence decay time of smaller primary aggregates and $\tau_2$ depicts the decay time for the larger suprastructures. Both the primary and the secondary aggregates are found to be the largest in case of 2 μM DMASBT. Moreover, the aggregates formed due to 4 μM DMASBT appear to be smaller compared to those formed due to 1 μM DMASBT. The decay profile of DMASBT in water could not be provided here since the fluorescence decay time of free DMASBT in water is very short and is out of the scope of the instrument resolution where the experiments were performed.[15] The decay profile of DMASBT appears along the lamp profile and thus is evident that its lifetime is less than 70 ps since the typical response time of the laser system was 70 ps.

The point to note is the primary interaction between the 1:2 complexes to form the nanotubes followed by the secondary interaction to form the nanotubular suprastructures.[2] The experimental observations indicate that there must be some critical concentration for the smaller aggregates, only after reaching that the later interactions begin. Probe concentration of 1 μM fails to supply enough number of the small aggregates. DMASBT concentration of 2 μM, however, achieves this success, and we witness both the primary and secondary aggregations. Higher probe concentration also slows down the formation of large aggregates. Presumably, the reason behind this is the reluctance of the nanotubes to aggregate through the secondary interactions because of concentrating on finishing up the primary process first. As the number of DMASBT molecules is greater in this case, the 1:2 guest host complexes are

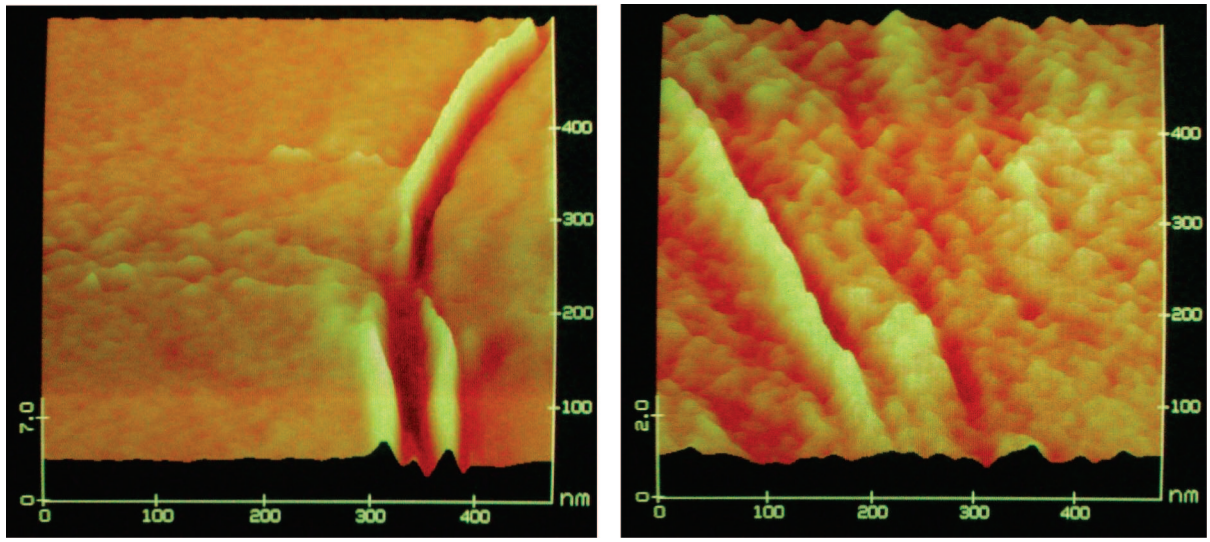


**Figure 7.** AFM micrographs showing the DMASBT (2 $\mu$M) induced nanotubular suprastructures developed at an α-CD concentration of 10 mM. The figure on the left shows the formation of larger aggregates and that on the right shows the formation of the comparatively smaller ones (as are reflected from the z-scale).

**SCHEME 2: Arrangement of the Nanocapsules to Form the Nanotubular Suprastructure**

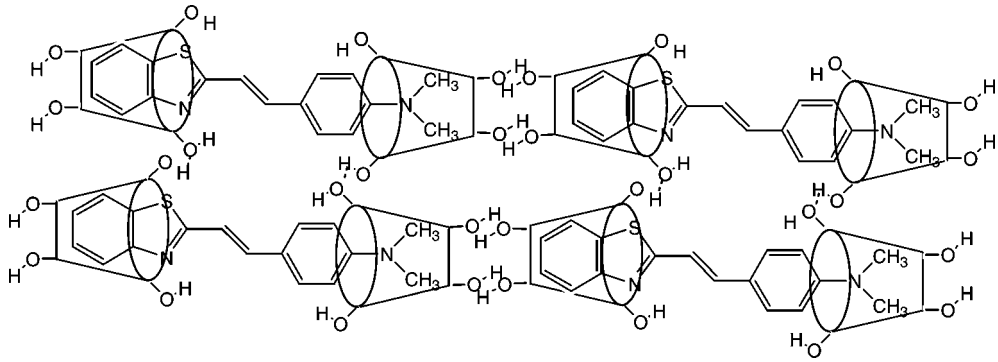

developed in higher numbers and only after proceeding in this process up to a considerable α-CD concentration range they incline toward the suprastructure development (as indicated by the fluorescence anisotropy).

Another explanation can stem from the anisotropy data. The motional restriction of the fluorophore is observed most in the case of 2 $\mu$M DMASBT. This may lead to supply enough time to the nanotubes to form hydrogen bonding with similar counterparts to form the aggregate. Whereas, in case of the other concentrations of DMASBT the molecular motion is not as restricted as in the former, which may not allow the hydrogen bonding to form so effectively as in the previous case. Consequently, the process might shed impact on the nanotubular suprastructure formation. To confirm the formation of the nanotubular suprastructures, we took the help of the atomic force microscopy (AFM) technique where the rods are visible clearly (Figure 7). α-CD is known to undergo self-aggregation forming nanosized spherical aggregates,[21] but for the development of the nanotubular suprastructures the system seeks the intervention of other molecules, mainly polymeric in nature, so that the CD aggregates can group together to form the nanotubes.

The nanotubular aggregates formed are found to be around 318 nm long and around 14 nm wide. α-CD has an inner diameter of 5.7 Å and a depth of 7.9 Å.[22] While getting encapsulated by the CD moieties from the two ends, because of the molecular dimensions DMASBT cannot move up to the bottom of the CD bucket. In other words, the two CDs on the two ends of DMASBT cannot approach face to face close enough to develop hydrogen bonding between the −OH groups on the rim. Thus, the capsules take a size a little more than the total size of two α-CD molecules (molecular dimensions were calculated using semiempirical AM1 method). On attainment of a critical concentration, somewhat similar to nucleation in polymerization process, each of those capsules aggregate parallel to each other in both directions to form rods 318 nm long. Moreover, an excess of DMASBT molecules slows down the process as they concentrate more on the primary interactions than the secondary ones. The $\pi$-cloud interactions among the DMASBT molecules help in the arrangement of the nanotubes to favor the aggregation (Scheme 2). That the interactions between the nanocapsules are primarily through hydrogen bonding can be examined by the effect of different concentrations of an alkali on the nanoaggregates. We performed similar experiments and observed a decrease in the fluorescence intensity of the TICT band of DMASBT with a concomitant red shift. This indicates that the hydroxyl groups on the rims of the cyclodextrins react with the $OH^-$ ions from the alkali and leaves $O^-$, thus decreasing the number of hydrogen bonds (see Figure 2 in Supporting Information). The probe molecule is experiencing more aqueous environment where the fluorescence quantum yield decreases with a red shift of the fluorescence maximum.[15]

## Conclusion

Through this work we have demonstrated a rare event of formation of nanotubular aggregates of α-CD induced by a compound (DMASBT) that has ICT character. The aggregation is found to be very much dependent on the probe concentration. The different phases of the formation of the host−guest complexes proceed through primary and secondary interactions. Molecules like DMASBT that only favor the 1:2 host−guest complexation seem to be potential candidates for the development of these kinds of suprastructures, which have huge importance in the field of selective drug delivery. Since the fluorescence yield of DMASBT is found to increase remarkably with change in polarity of the environment, it can also be used as very good biosensor. We look for its further applications in biological as well as pharmaceutical research.

**Acknowledgment.** This work was supported by the Department of Science and Technology, Govt. of India (SR/FTP/CS-114/2005) Birla Institute of Technology and Science, Pilani. The authors owe acknowledgement to Dr. Chandra Sekhar, Director, CEERI, Pilani, India for granting permission to work with the AFM facility of the institute and Professor N. Chattopadhyay of the Department of Chemistry, Jadavpur University, Calcutta, India for his permission to use the time-resolved fluorescence setup. Authors owe their special thanks to both of the reviewers whose comments helped them to give the presentation a better shape.

**Supporting Information Available:** Figure 1. Optimized geometry of trans-2-[4-(dimethylamino)styryl]benzothiazole (DMASBT). Width of DMASBT (24−21), 5.034 Å, width of DMASBT (30−28), 4.985 Å, and length of DMASBT (22−34), 15.584 Å. Figure 2. Fluorescence spectra of DMASBT ($1 \times 10^{-5}$ M) in 10 mM α-CD solution and different concentrations of NaOH (from 0 to 32 mM). This information is available free of charge via the Internet at http://pubs.acs.org.

## References and Notes

(1) (a) Mayer, B.; Köhler, G.; Rasmussen, S. *Phys. Rev.* **1997**, *E55*, 4489–4499. (b) Schnur, J. M. *Science* **1993**, *262*, 1669–1676. (c) Stupp, S. I.; LeBonheur, V.; Walker, K.; Li, L. S.; Huggins, K. E.; Keser, M.; Amstutz, A. *Science* **1997**, *276*, 384–389. (d) Sleytr, U. B.; Pum, D.; Sara, M. *Adv. Biophys.* **1997**, *34*, 71–79. (e) Allara, D. L. *Nanofabrication and Biosystems*; Koch, H. C., ; Jelinsky, L. W., ; Graighead, H. C., Eds.; Cambridge University Press: Cambridge, 1996.

(2) (a) Li, G.; McGown, L. B. *Science* **1994**, *264*, 249–251. (b) Pistolis, G.; Malliaris, A. *J. Phys. Chem.* **1996**, *100*, 15562–15568. (c) Wu, A.; Shen, X.; He, Y. *J. Colloid Interface Sci.* **2006**, *297*, 525–533. (d) Wu, A.; Shen, X.; He, Y. *J. Colloid Interface Sci.* **2006**, *302*, 87–94.

(3) (a) French, D. *Adv Carbohydr. Chem.* **1957**, *12*, 189–260. (b) Saenger, W. *Angew. Chem., Int. Ed. Engl.* **1980**, *19*, 344–362.

(4) Szetli, J. *Cyclodextrin Technology*; Davis, J. E. D., Ed.; Kluwer Academic: Dordrecht, 1988.

(5) (a) Schneider, H. J.; Hacket, F.; Rudiger, V.; Ikeda, H. *Chem. Rev* **1998**, *98*, 1755–1785. (b) Breslow, R.; Dong, S. D. *Chem. Rev.* **1998**, *98*, 1997–2012. (c) Engeldinger, E.; Armspach, D.; Matt, D. *Chem. Rev.* **2003**, *103*, 4147–4173.

(6) (a) Schneider, H. J.; Sangwan, N. K. *Angew. Chem., Int. Ed. Engl.* **1987**, *26*, 896–897. (b) Purkayastha, P.; Chattopadhyay, N. *J. Mol. Struct.* **2001**, *570*, 145–152. (c) Haldar, B.; Mallick, A.; Purkayastha, P.; Burrows, H. D.; Chattopadhyay, N. *Indian J. Chem.* **2004**, *43A*, 2265–2273.

(7) (a) Klingert, B.; Rihs, G. *Organometallics* **1990**, *9*, 1135–1141. (b) Wenz, G.; Keller, B. *Angew. Chem., Int. Ed.* **1992**, *31*, 197–199. (c) Girardeau, T. E.; Leisen, J.; Beckham, H. W. *Macromol. Chem. Phys.* **2005**, *206*, 998–1005. (d) Ceccato, M.; Nostro, P. L.; Baglioni, P. *Langmuir* **1997**, *13*, 2436–3439.

(8) Yang, G.-F.; Wang, H.-B.; Yang, W.-C.; Gao, D.; Zhan, C.-G. *J. Chem. Phys.* **2006**, *125*, 111104−1111104−4.

(9) (a) He, Y.; Fua, P.; Shen, X.; Gao, H. *Micron* **2007**, . doi:10.1016/j.micron.2007.06.017. (b) Miyake, K.; Yasuda, S.; Harada, A.; Sumaoka, J.; Komiyama, M.; Shigekawa, H. *J. Am. Chem. Soc.* **2003**, *125*, 5080–5085.

(10) Hernández-Pescacio, J.; Garza, C.; Banquy, X.; Díaz-Vergara, N.; Amigo, A.; Ramos, S.; Castillo, R.; Costas, M.; Piñeiro, Á. *J. Phys. Chem. B* **2007**, *111*, 12625–12630.

(11) (a) Harada, A.; Li, J.; Kamachi, M. *Macromolecules* **1994**, *27*, 4538–4543. (b) Ceccato, M.; Nostro, P. L.; Rossi, C.; Bonechi, C.; Donati, A.; Baglioni, P. *J. Phys. Chem. B* **1997**, *101*, 5094–5099.

(12) Park, C.; Lee, I. H.; Lee, S.; Song, Y.; Rhue, M.; Kim, C. *Proc. Nat. Acad. Sci. U.S.A.* **2006**, *103*, 1199–1203.

(13) (a) Rotkiewicz, K.; Grellmann, K. H.; Grabowski, Z. R. *Chem. Phys. Lett.* **1973**, *19*, 315–318. (b) Grabowski, Z. R.; Rotkiewicz, K.; Siemiarczuk, A.; Cowley, D. J.; Baumann, W. *Nouv. J. Chim.* **1979**, *3*, 443–454.

(14) (a) Jiang, Y.-B. *Appl. Spectrosc.* **1994**, *48*, 1043–1179. (b) Kundu, S.; Maity, S.; Bera, S. C.; Chattopadhyay, N. *J. Mol. Struct.* **1997**, *405*, 231–238. (c) Krishnamoorthy, G.; Dogra, S. K. *Chem. Phys. Lett.* **2000**, *323*, 234–242. (d) Raju, B. B.; Costa, M. B. *Phys. Chem. Chem. Phys.* **1999**, *1*, 5029–5034. (e) Al-Hassan, K. A.; Khanfer, M. F. *J. Fluoresc.* **1998**, *8*, 139–152.

(15) (a) Fayed, T. A.; Ali, S. S. *Spectrosc. Lett.* **2003**, *36*, 375–386. (b) Saha, S. K.; Purkayastha, P.; Das, A. B. *J. Photochem. Photobiol. A: Chem.* **2008**, *195*, 368–377.

(16) (a) Tønnensen, H. H.; Másson, M.; Loftsson, T. *Int. J. Pharm.* **2002**, *244*, 127–135. (b) Li, X.-S.; Liu, L.; Guo, Q.-X.; Chu, S.-D.; Liu, Y.-C. *Chem. Phys. Lett.* **1999**, *307*, 117–120.

(17) Connors K. A. *The Measurement of Molecular Complex Stability*; Wiley: New York, 1987.

(18) Shen, X.; Belletête, M.; Durocher, G. *Chem. Phys. Lett.* **1998**, *298*, 201–210.

(19) Chakrabarty, A.; Mallick, A.; Haldar, B.; Das, P.; Chattopadhyay, N. *Biomacromolecules* **2007**, *8*, 920–927.

(20) Small, E. W.; Isenberg, I. *Biopolymers* **2004**, *16*, 1907–1928.

(21) Coleman, A. W.; Nicolis, I.; Keller, N.; Dalbiez, J. P. *J. Inclusion Phenom. Mol. Recognit. Chem.* **1992**, *13*, 139–143.

(22) Li, S.; Purdy, W. C. *Chem. Rev.* **1992**, *92*, 1457–1470.

JP8018952